DECLASSIFIED

UCRL 211 Rev

Cy 2

[redacted]

UNIVERSITY OF CALIFORNIA

Radiation Laboratory

TWO-WEEK LOAN COPY

This is a Library Circulating Copy which may be borrowed for two weeks. For a personal retention copy, call Tech. Info. Division, Ext. 5545

BERKELEY, CALIFORNIA

DISCLAIMER

This document was prepared as an account of work sponsored by the United States Government. While this document is believed to contain correct information, neither the United States Government nor any agency thereof, nor the Regents of the University of California, nor any of their employees, makes any warranty, express or implied, or assumes any legal responsibility for the accuracy, completeness, or usefulness of any information, apparatus, product, or process disclosed, or represents that its use would not infringe privately owned rights. Reference herein to any specific commercial product, process, or service by its trade name, trademark, manufacturer, or otherwise, does not necessarily constitute or imply its endorsement, recommendation, or favoring by the United States Government or any agency thereof, or the Regents of the University of California. The views and opinions of authors expressed herein do not necessarily state or reflect those of the United States Government or any agency thereof or the Regents of the University of California.

DECLASSIFIED

SECRET

UCRL-211 (Revised)

Physics-General

Copy 2

UNIVERSITY OF CALIFORNIA

Radiation Laboratory

CLASSIFICATION CANCELLED
BY AUTHORITY OF THE DECLASSIFICATION BRANCH USAEC per Crash List # 11
BY B Foskett 6-4-56
SIGNATURE OF THE PERSON MAKING THE CHANGE DATE

Contract No. W-7405-eng-48

[redacted]

CLASSIFICATION CANCELLED BY AUTHORITY OF THE DECLASSIFICATION COMMITTEE

Kinetic Energy Release in Fission of U^{238}, U^{235}, Th^{232}, and Bi^{209} by High Energy Neutrons

J. Jungerman and S. C. Wright

December 30, 1948

Berkeley, California

DECLASSIFIED

Standard Distribution	Copy Nos.
Argonne National Laboratory	1-8
Armed Forces Special Weapons Project	9
Atomic Energy Commission, Washington	10-11
Battelle Memorial Institute	12
Brookhaven National Laboratory	13-20
Bureau of Ships	21
Carbide & Carbon Chemicals Corp. (K-25 Plant)	22-25
Carbide & Carbon Chemicals Corp. (Y-12 Plant)	26-29
Columbia University (Dunning)	30
General Electric Company, Richland	31-34
Hanford Operations Office	35
Iowa State College	36
Knolls Atomic Power Laboratory	37-40
Los Alamos	41-43
Mound Laboratory	44-45
National Bureau of Standards	46-47
Naval Radiological Defense Laboratory	48
NEPA Project	49
New York Operations Office	50-51
North American Aviation, Inc.	52
Oak Ridge National Laboratory	53-60
Patent Advisor, Washington	61
Sandia Base	62-63
Technical Information Division, OROO	64-78
UCLA Medical Research Laboratory (Warren)	79
University of California Radiation Laboratory	80-84
University of Rochester	85-86
Total	86

Information Division
Radiation Laboratory
University of California
Berkeley, California

DECLASSIFIED

Kinetic Energy Release in Fission of U^{238}, U^{235}, Th^{232}, and Bi^{209} by High Energy Neutrons

J. Jungerman and S. C. Wright

Radiation Laboratory, Department of Physics,
University of California, Berkeley, California

Abstract

The ionization produced by single fission fragments was observed in an ionization chamber using electron collection. If fission is induced by 90 Mev neutrons, the distribution of kinetic energy of the fission fragment versus the number of fragments is found to have a single peak in contrast to the double-peaked curve corresponding to the fission made by thermal neutrons. Fission induced by 45 Mev neutrons gives a distribution in which two peaks appear. The dip between the two peaks is about twenty percent of the height of the peaks. The mean kinetic energy is found to be 80 ± 2 Mev for U^{238}, 83 ± 1.5 Mev for U^{235}, 82 ± 2 Mev for Th^{232}, and 71 ± 2 Mev for Bi^{209} in the case of fission produced by 90 Mev neutrons. The mean kinetic energy is 79 ± 3 Mev for U^{238} and 84 ± 3 Mev for Th^{232} if 45 Mev neutrons are used. The most probable kinetic energy of the fragment is 83 Mev for U^{238}, 80 Mev for U^{235}, 83 Mev for Th^{232}, and 75 Mev for Bi^{209} in the case of fission produced by 90 Mev neutrons. The bearing of these observations on the mechanism of fission is discussed.

DECLASSIFIED

Kinetic Energy Release in Fission of U^{238}, U^{235}, Th^{232}, and Bi^{209} by High Energy Neutrons

J. Jungerman and S. C. Wright

Radiation Laboratory, Department of Physics
University of California, Berkeley, California

Introduction

The kinetic energy release occurring in fission induced by low energy neutrons has been studied by Jentschke[1], Flammerfeld et al[2], Brolley[3], Deutsch and Ramsey[4], and Fowler and Rosen[5]. The results of these experiments show that the distribution of the kinetic energy of single fragments versus the number of fragments consists of two peaks. The energy distribution is consistent with the mass distribution of the fragments known from chemical evidence and the assumption that the kinetic energy observed is derived only from the coulomb repulsion of two charged fragments[4]. The object of the experiment reported here was to investigate the kinetic energy distribution of single fragments produced in fission caused by 90 Mev and 45 Mev neutrons and the influence of the increased excitation on the mean fragment energy. To this aim the kinetic energy of single fragments was measured by the use of an ionization chamber, a linear amplifier, and a camera for photographically recording pulse heights on an oscilloscope.

Experimental

Figure 1 shows a diagram of the ionization chamber employed. Each target plate had a foil spot welded to its surface. This foil was covered with the element under investigation. The foils in the cases of uranium and thorium were prepared by painting solutions of the nitrates on 1 mil aluminum and baking at 500^{0} C until the oxides were formed[6]. The amount of material never exceeded 3×10^{-5} gms/cm^2. Foils surfaced with 5×10^{-5} gms/cm^2 of bismuth were prepared by evaporation of the metal on 1 mil aluminum.

The grids G consisted of 3 mil nichrome wire 50 mils apart. The chamber was filled with pure argon at a pressure of 160 cm of Hg. The electrodes were so arranged

DECLASSIFIED

that at this gas pressure the distance between the target plate T and the grid G was greater than the range of the fragments. The voltages were such that a stronger electric field existed between the grid and collecting plate than between the grid and the target plate. This tended to funnel the lines of force through the spaces in the grid and to prevent electrons from being collected at the grid.

Charged particles produced by the neutron beam in the chamber electrodes and gas caused spurious ionization pulses to be superimposed on the pulses from the fission fragments. In order to reduce this background ionization as much as possible, the chamber walls and electrodes were made as thin as practicable. The neutron beam entered through a 2 mil stainless steel window, traversed a 1 mil aluminum foil with the sample on it, the grid, and finally a 0.5 mil aluminum foil collecting plate. It then passed on through a similar unit of two plates and a grid. There were four such units in all. The last usually contained a sample of U^{235} for calibration purposes.

The electronic circuit is shown schematically in Fig. 2. This arrangement was employed in order to discriminate both electronically during the experiment and visually during the film analysis, against pulses caused by high energy neutron reactions in the argon and chamber plates along the path of the beam. A pulse from the ionization chamber was amplified and then fed directly onto the oscilloscope deflection plates via a 2 μ sec delay line. Another amplifier out-put fed the pulse to the discriminator housed in the intensifier and sync-generator chassis. If the pulse was high enough to be accepted by the discriminator an intensifying pulse travelled to the oscilloscope grid. At the same time the pulse initiated a 5 μ sec sweep on the oscilloscope. In this way it was possible to see the start of the trace, the pulse rise, and the first part of the decay. Figure 3 shows the form of a typical pulse. The distance x in the figure was taken to be the pulse height. Any pulse in which the initial base line and the pulse rise form differed from that in Fig. 3 was rejected. Figure 4 is an exaggerated example of such a rejected pulse. These unsatisfactory pulses were assumed to be due to a combination of fission fragment ionization and ionization produced by neutron reactions in the electrodes and gas. Their

number never amounted to more than 5 percent of the total. The discriminator on the intensifier circuit prevented a large number of low energy pulses from being recorded. This considerably simplified the photographic analysis and made the readings more accurate. The amplifier was of the fast rise time variety stabilized by inverse feed back. The fission pulses had a rise time of 1.5 sec and decayed to 1/e in 10 μ sec. A fast rise time pulse generator connected when required to the grid of the chamber checked the linearity and amplification of the equipment on the different bombardments. Calibration pulses from the pulse generator were used before and after each run.

The pulses on the Dumont 248 oscilloscope were photographed with a camera using continuously moving 35 mm Super XX film. All pulse heights were measured on the same microfilm viewer.

In order to check the resolution of the apparatus and to calibrate the energy scale, the usual experimental arrangement in the ionization chamber was to have a sample of U^{235} on plate A and samples of the element under investigation on plate B (see Fig. 1). Immediately before or after a cyclotron run a fission fragment energy distribution was made with slow neutrons on U^{235} using the same chamber gas and the same setting of the amplifier and oscilloscope. The resolution of the chamber was considered satisfactory if the U^{235} (slow n, fission) fragment energy distribution agreed with the curves of Deutsch and Ramsey[4] within statistics. The absolute energy scale was determined by comparison of the Deutsch and Ramsey U^{235} distribution (assumed correct) to the U^{235} (slow n, fission) curves obtained in this experiment. The latter were in turn used to obtain the energy scale for the high energy neutron fission fragment distributions. Since the cyclotron magnetic field was different at the bombardment and calibration positions a check of the effect of position on the amplification of the apparatus was made by making slow neutron runs at both locations. The pulse height average was found to be 3 percent higher at the bombardment position. This factor has been included in the energy scale calculation.

The high energy neutrons used in these experiments were formed by bombardment of a 3/8 in. Be target with 190 Mev or 95 Mev deuterons. See Serber[7] for the distribution

in energy of neutrons so produced. The most probable neutron energies in the two cases are 90 Mev and 45 Mev respectively. This is the meaning of the terms 90 Mev and 45 Mev neutrons as used in this paper. Ra - Be enclosed in paraffin provided a thermal neutron source.

Results

Figures 5, 6, 7, 8, 9, and 10 show the actual histograms of the fragment energy distributions of U^{238}, U^{235}, Th^{232}, and Bi^{209}, obtained in the experiment. Figure 11 shows a typical slow neutron calibration histogram. Figures 12 and 13 show the probable distributions corresponding to these histograms. Each curve is normalized to 1000 pulses. In order to check that all pulses corresponding to 40 Mev or more were due to the active material, cyclotron runs were made with an aluminum blank of the same thickness, 1 mil, as that supporting the sample. These runs showed that the number of pulses corresponding to fission fragments of 40 Mev or higher were negligible. For fission induced by 90 Mev neutrons it is found that the mean fragment energy is 80 $\pm$ 2 Mev for U^{238}, 83 $\pm$ 1.5 Mev for U^{235}, 82 $\pm$ 2 Mev for Th^{232}, and 71 $\pm$ 2 Mev for Bi^{209}. The energy spread at one half maximum is 40 Mev for U^{238}, 38 Mev for U^{235}, 44 Mev for Th^{232}, and 24 Mev for Bi^{209}. The energy scale for the figures was obtained by comparison of the slow neutron calibration curve for each run with the curve of Deutsch and Ramsey[4]. This checked within the experimental error by measuring the pulses produced in our apparatus by the alpha particles of U^{234}. For fission induced by 45 Mev neutrons two peaks appeared in the energy distributions. For Th^{232} the maxima are at 73 Mev and 104 Mev, for U^{238} at 68 Mev and 89 Mev. The mean fragment energy is 84 $\pm$ 3 Mev for Th^{232} and 79 $\pm$ 3 Mev for U^{238}. The form of the distributions should be accurate within statistics.

Discussion

The foregoing assumes that the number of ion pairs is proportional to the energy of the fission fragments producing them.

If the fission is assumed to be binary, as is most probable, this experiment shows

that the mode of fission induced by 90 Mev neutrons that gives equal kinetic energies to the fragments is the most probable one in contrast to the results of thermal neutron fission. The mean kinetic energy of the fragments is, in the case of U^{235}, only 5 Mev higher than that from fission induced by slow neutrons. The kinetic energy of the incident neutron must therefore be accounted for by some other mechanism than appearance in the kinetic energy of the fission fragments[8].

Goeckermann and Perlman[9] have investigated fission products formed from bismuth by 200 Mev deuterons. They find that the mass-number distribution has a maximum at about 100 mass units. This indicates a loss of approximately 10 neutrons from the compound nucleus before fission takes place.

The following mechanism is tentatively suggested for the fission process caused by high energy neutrons. It is not unique but may represent a limiting case to which the actual process approximates. See Fig. 14. The compound nucleus Z^{A+1*} formed from the nucleus Z^{A} by capture of a high energy neutron evaporates J neutrons until its energy A above the ground level is less than the binding energy C of a neutron to the nucleus Z^{A+1-J*}. The mean lives of fission and gamma emission are long compared with that for neutron emission where the latter is energetically possible and they will be unimportant during the initial evaporation process. Fission may be expected to have a threshold at some energy B above the ground level. If the level A is above B, fission may occur and compete with gamma emission, if it is below B only gamma emission is possible. Thus in general when the level A is reached, two processes, gamma radiation and fission are important for the removal of the remaining excitation. The relative probabilities of A being above or below the fission threshold B should be proportional to the number of levels available in the two regions. According to this picture fission should occur in a relatively unexcited compound nucleus in competition with gamma emission and therefore exhibit a cross section for fission less than the geometrical with fluctuations from element to element. This is in agreement with the following. Recent measurements by Jungerman, Kelly, Wiegand, and Wright give the absolute fission cross section for 90 Mev neutrons on uranium and thorium to be 1.4 barns and 1.0

barns respectively. In each case the cross section is less than one half the geometric cross section and also the two values differ considerably.

In the high energy neutron fission of U^{235} the mean kinetic energy of the fragments is only slightly higher than that of the thermal neutron fission fragments. For Bi^{209} the mean fragment energy is 0.91 times the latter. It was pointed out in the introduction that the energy distribution of the fragments in thermal neutron fission is consistent with their known mass distribution under the assumption that the kinetic energy observed is derived from the coulomb repulsion of two charged fragments. Since it has been suggested above that in high energy neutron fission the actual division of the nucleus only occurs in a relatively unexcited state, in fact of the same order of excitation as in the thermal neutron case, the high energy case should agree with a similar treatment. This can be easily checked for symmetrical fission with the crude model of Fig. 15. At the moment of separation the two fragments are assumed spherical in shape with a uniform distribution of charge and radii $R = r_0 \times A^{1/3}$ where A is the mass number of the fragment and r_0 is a constant. Also the charge of the fragments is assumed proportional to their mass. Under these conditions the coulomb potential energy E_c at the moment of separation will be

$$E_c = \frac{(Z_1 Z_2)\, e^2}{r_0 (A_1^{1/3} + A_2^{1/3})}$$

and for symmetrical fission

$$E_{c,s} = \frac{(Z_1\, e)^2}{2\, r_0 (A_1)^{1/3}} = \frac{(Z/2\, e)^2}{2\, r_0 \left(\frac{A - J + 1}{2}\right)^{1/3}}$$

Comparison of $E_{c,s}$ for 90 Mev neutrons on Bi^{209} and on U^{235} and placing J equal to 10 gives the ratio 0.88 which agrees moderately well with the experimental value 0.94 ± 0.04 considering the model used.

The fragment energy distributions obtained by the use of 45 Mev neutrons are interesting in that they exhibit the transition region between single and double peaked distributions

characteristic of fission with 90 Mev and slow neutrons respectively. However the actual energy distribution of the neutrons incident upon the fissionable material in this case has a width at half maximum of approximately 40 Mev so that it is impossible at present to say in what energy region the transition occurs.

Acknowledgements

We wish to thank C. Wiegand for some electronic equipment and for many valuable suggestions during the course of this work. We are deeply indebted to Prof. E. Segrè for suggesting this problem and for many stimulating discussions throughout the course of the investigation, and to Prof. Fermi for discussion of the fission mechanism. Thanks are also due the 184" cyclotron crew for valuable cooperation.

References

1. W. Jentschke, Zeits. f. Physik 120, 165 (1943).

2. A. Flammersfeld, Zeits. f. Physik 120, 450 (1943).

3. J. E. Brolley, CN 1840.

4. M. Deutsch and Ramsey, LADC 257.

5. J. L. Fowler and L. Rosen, Phys. Rev. 72, 926 (1947).

6. T. Jorgenson, MDDC 467.

7. R. Serber, Phys. Rev. 72, 1008 (1947).

8. According to M. L. Goldberger, Phys. Rev. 74, 1269 (1948) the average excitation a nucleus receives from a collision with a 90 Mev neutron is appreciably less than 90 Mev.

9. R. H. Goeckermann and I. Perlman, Phys. Rev. 73, 1127 (1948).

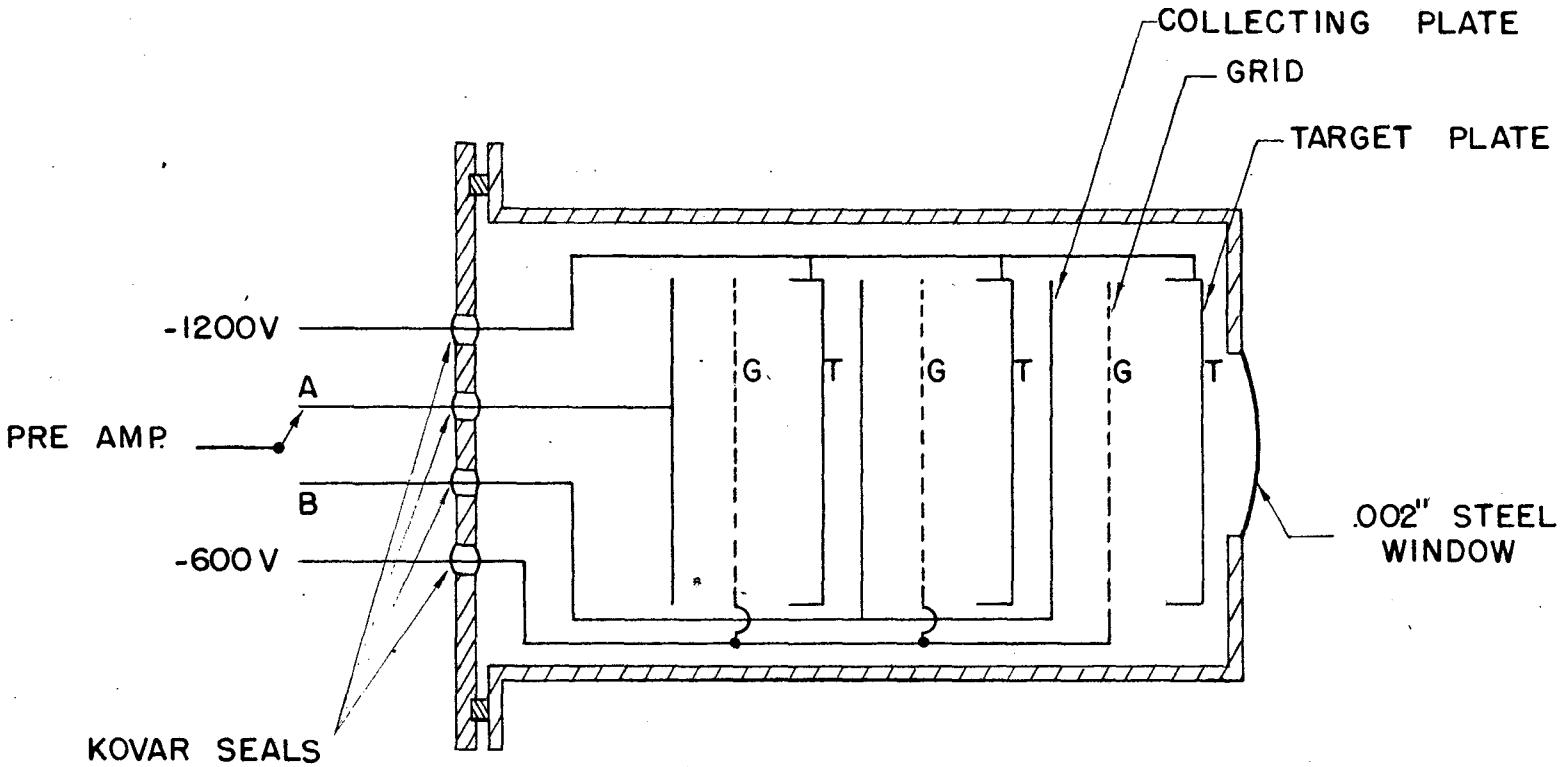
COLLECTING PLATE
GRID
TARGET PLATE
-1200V
A
PRE AMP.
B
-600 V
G
T
G
T
G
T
.002" STEEL WINDOW
KOVAR SEALS

FIG.1
13107-1

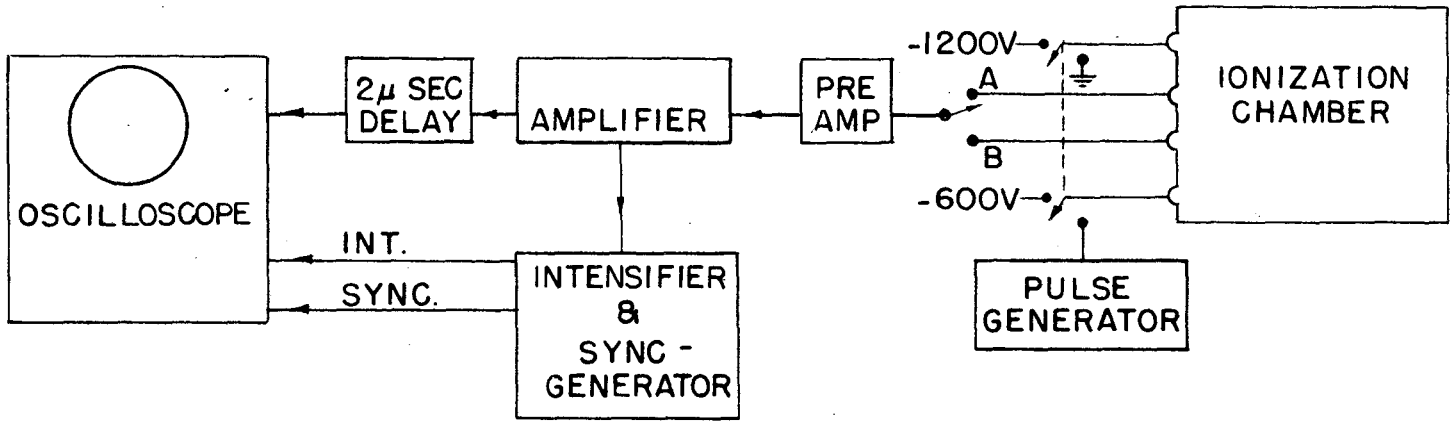
OSCILLOSCOPE
2μ SEC DELAY
AMPLIFIER
PRE AMP
-1200V
A
B
-600V
IONIZATION CHAMBER
INT.
SYNC.
INTENSIFIER & SYNC - GENERATOR
PULSE GENERATOR

FIG. 2

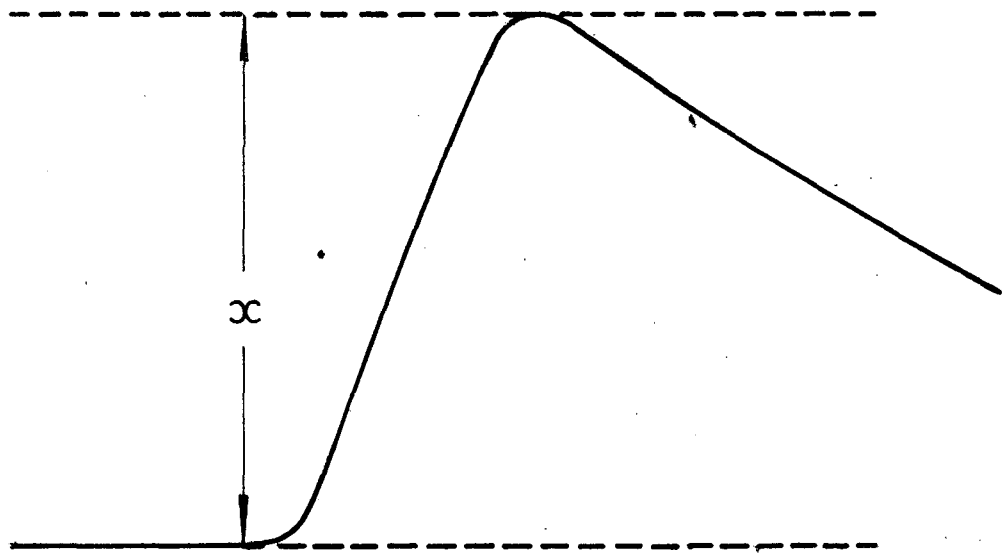

FIG. 3
13109-1

FIG. 4

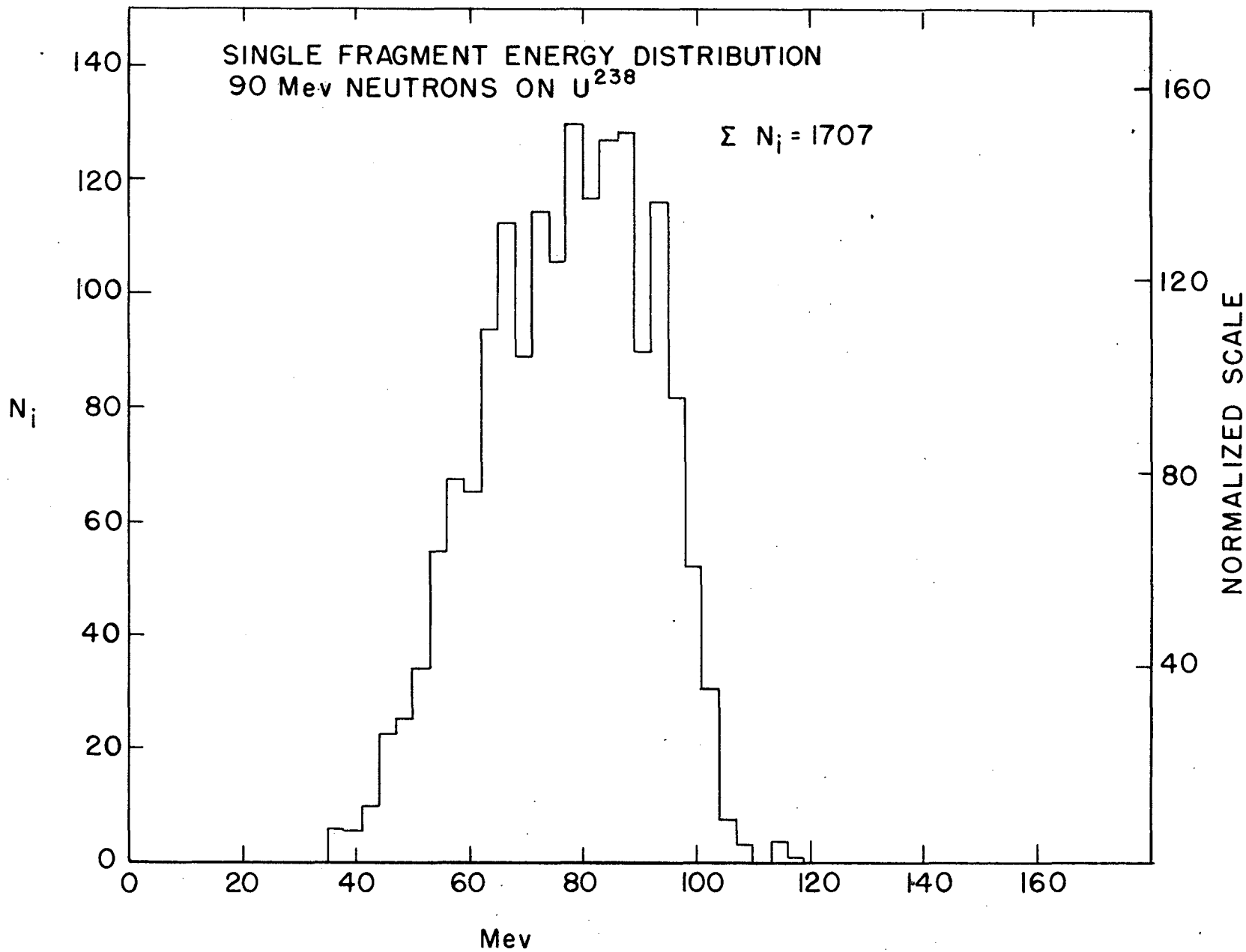
SINGLE FRAGMENT ENERGY DISTRIBUTION
90 Mev NEUTRONS ON U238
Σ Ni = 1707
Ni
NORMALIZED SCALE
Mev
0
20
40
60
80
100
120
140
160

FIG. 5

13211-1

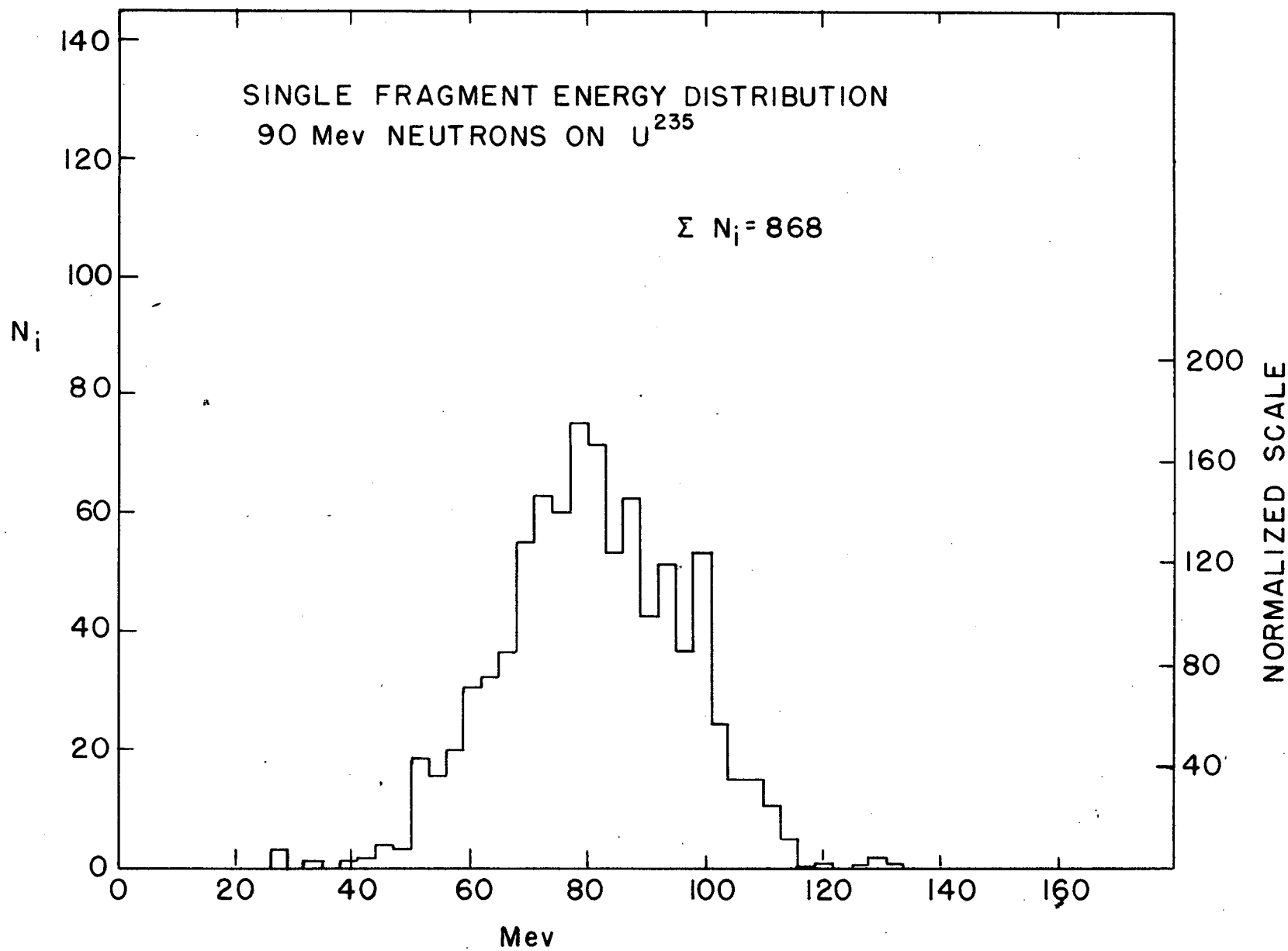
SINGLE FRAGMENT ENERGY DISTRIBUTION
90 Mev NEUTRONS ON U235
Σ Ni = 868
Ni
NORMALIZED SCALE
Mev
0
20
40
60
80
100
120
140
160
200

FIG. 6

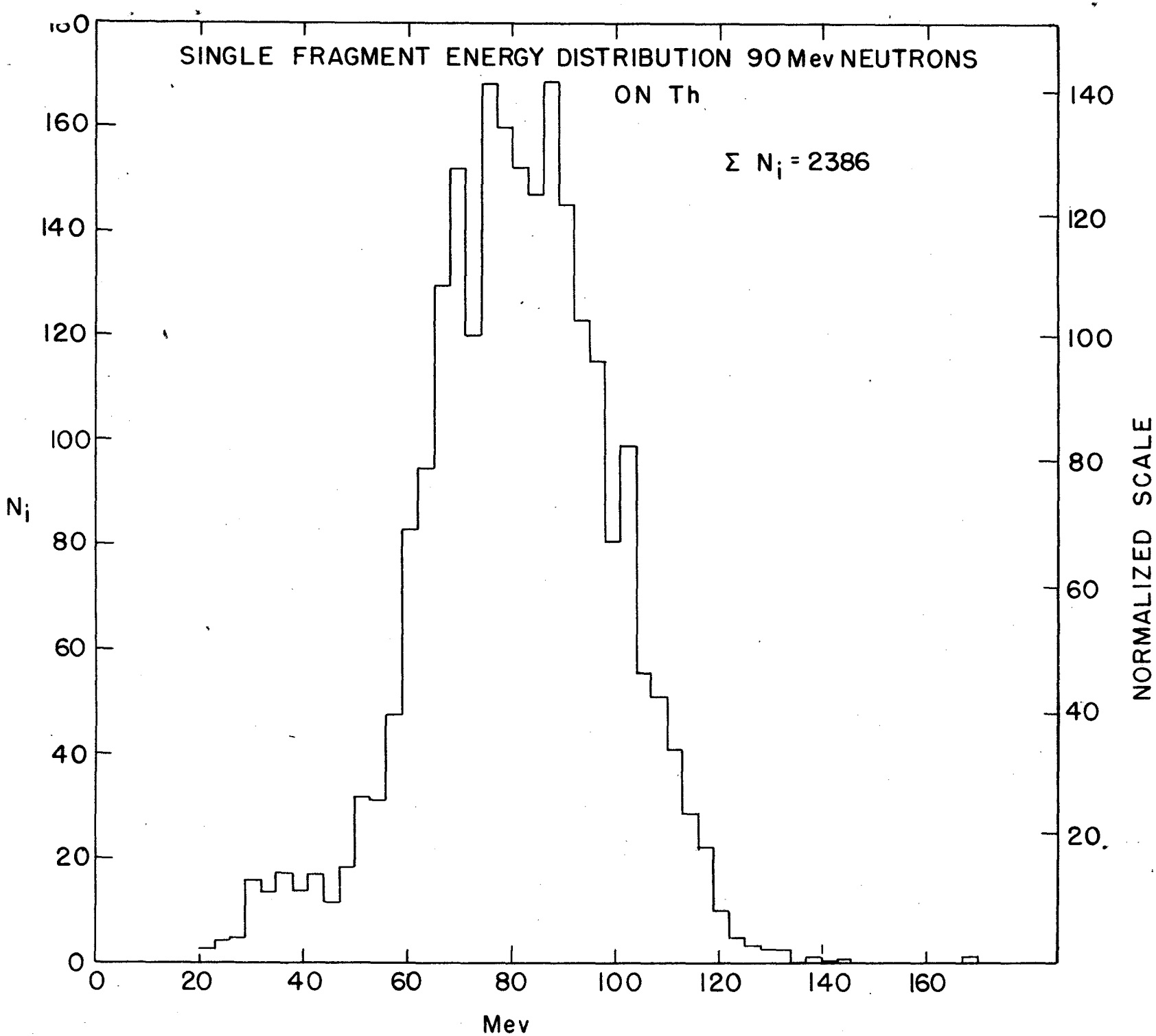

FIG. 7

13115-107

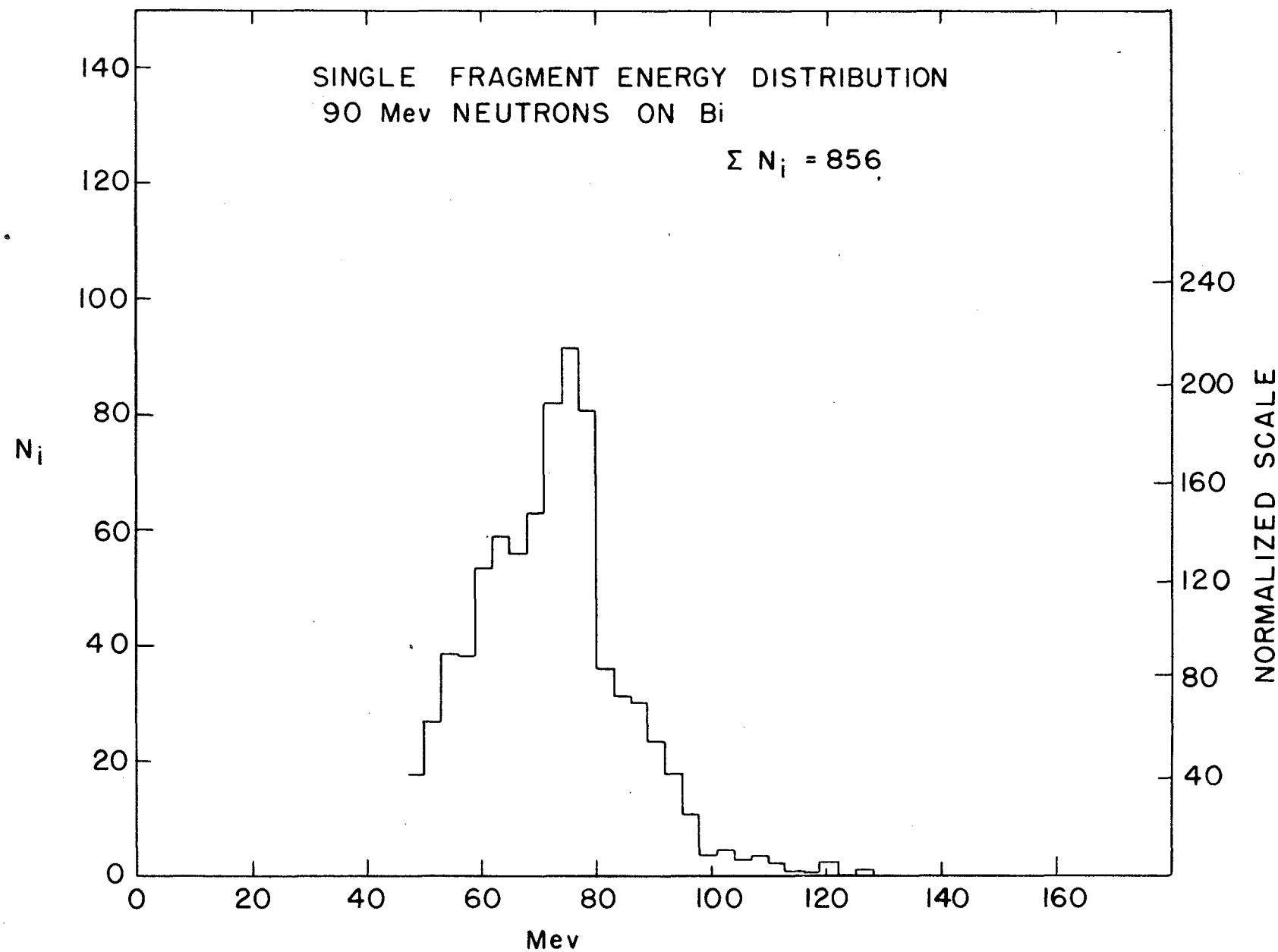
SINGLE FRAGMENT ENERGY DISTRIBUTION
90 Mev NEUTRONS ON Bi
Σ N_i = 856
N_i
0
20
40
60
80
100
120
140
Mev
0
20
40
60
80
100
120
140
160
NORMALIZED SCALE
40
80
120
160
200
240

FIG. 8

13212-1

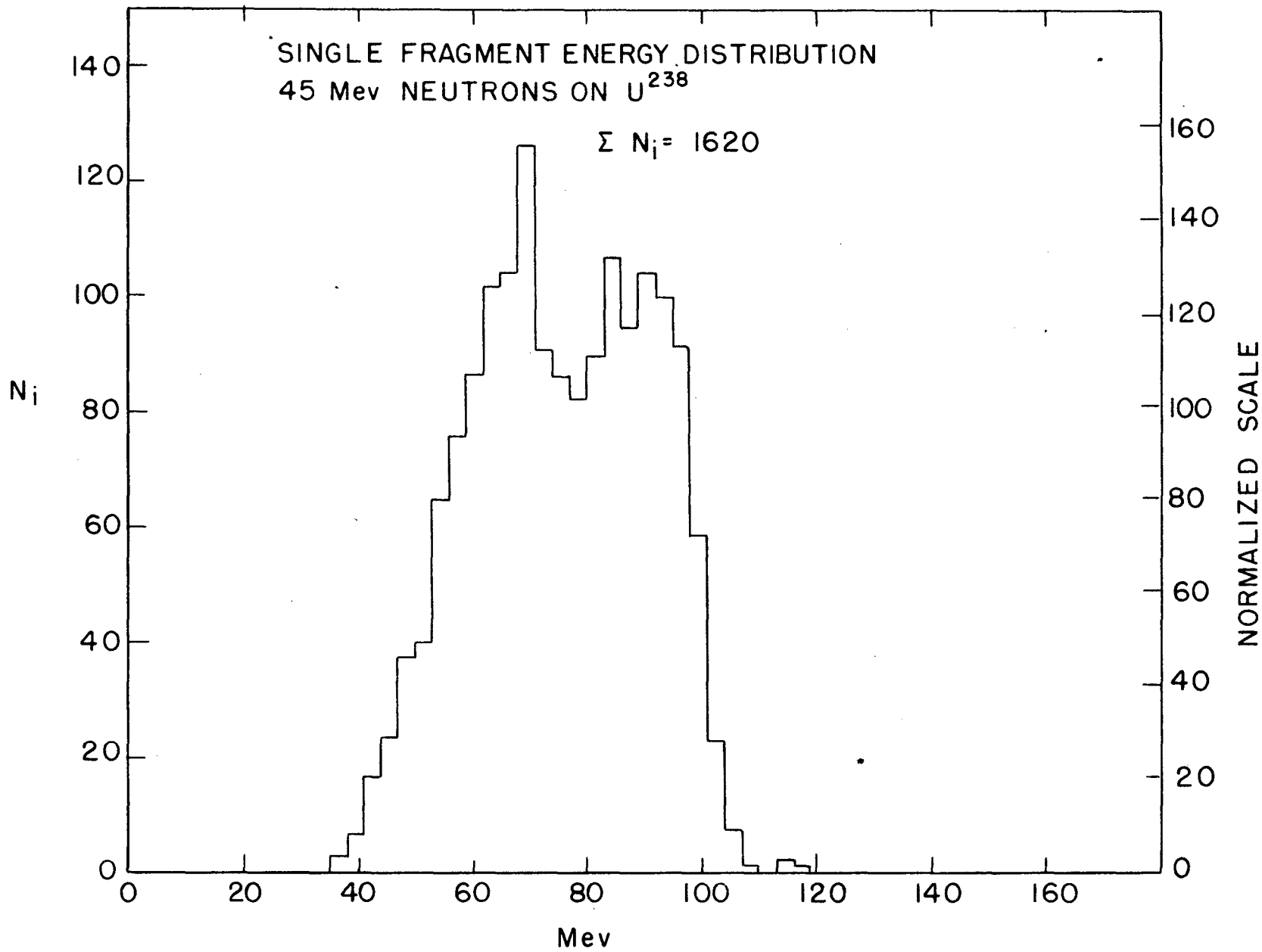
SINGLE FRAGMENT ENERGY DISTRIBUTION
45 Mev NEUTRONS ON U238
Σ Ni = 1620
Ni
NORMALIZED SCALE
Mev
0
20
40
60
80
100
120
140
160

FIG. 9

13213-1

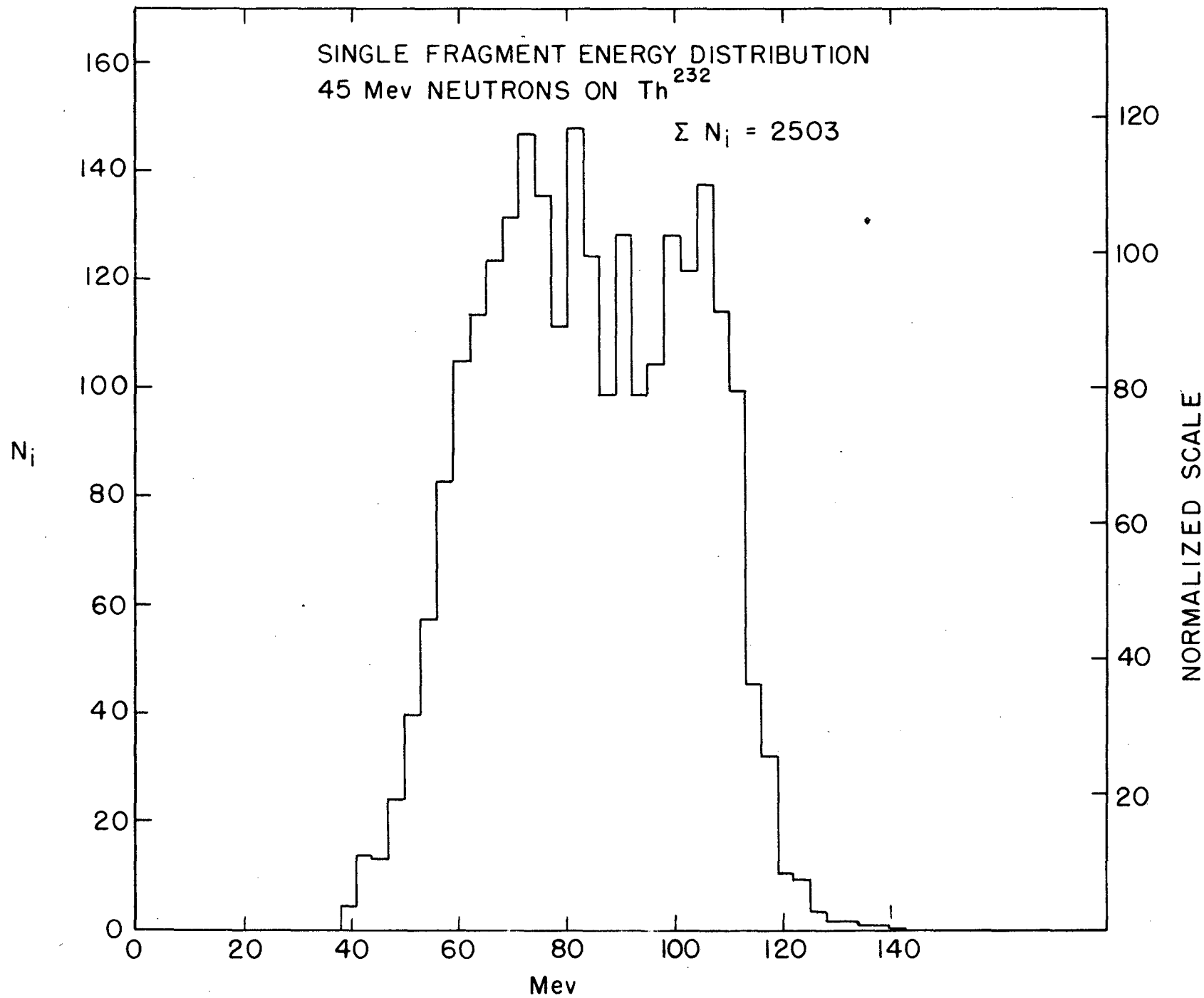
SINGLE FRAGMENT ENERGY DISTRIBUTION
45 Mev NEUTRONS ON Th232
Σ Ni = 2503
Ni
NORMALIZED SCALE
Mev
0
20
40
60
80
100
120
140
160

FIG. 10

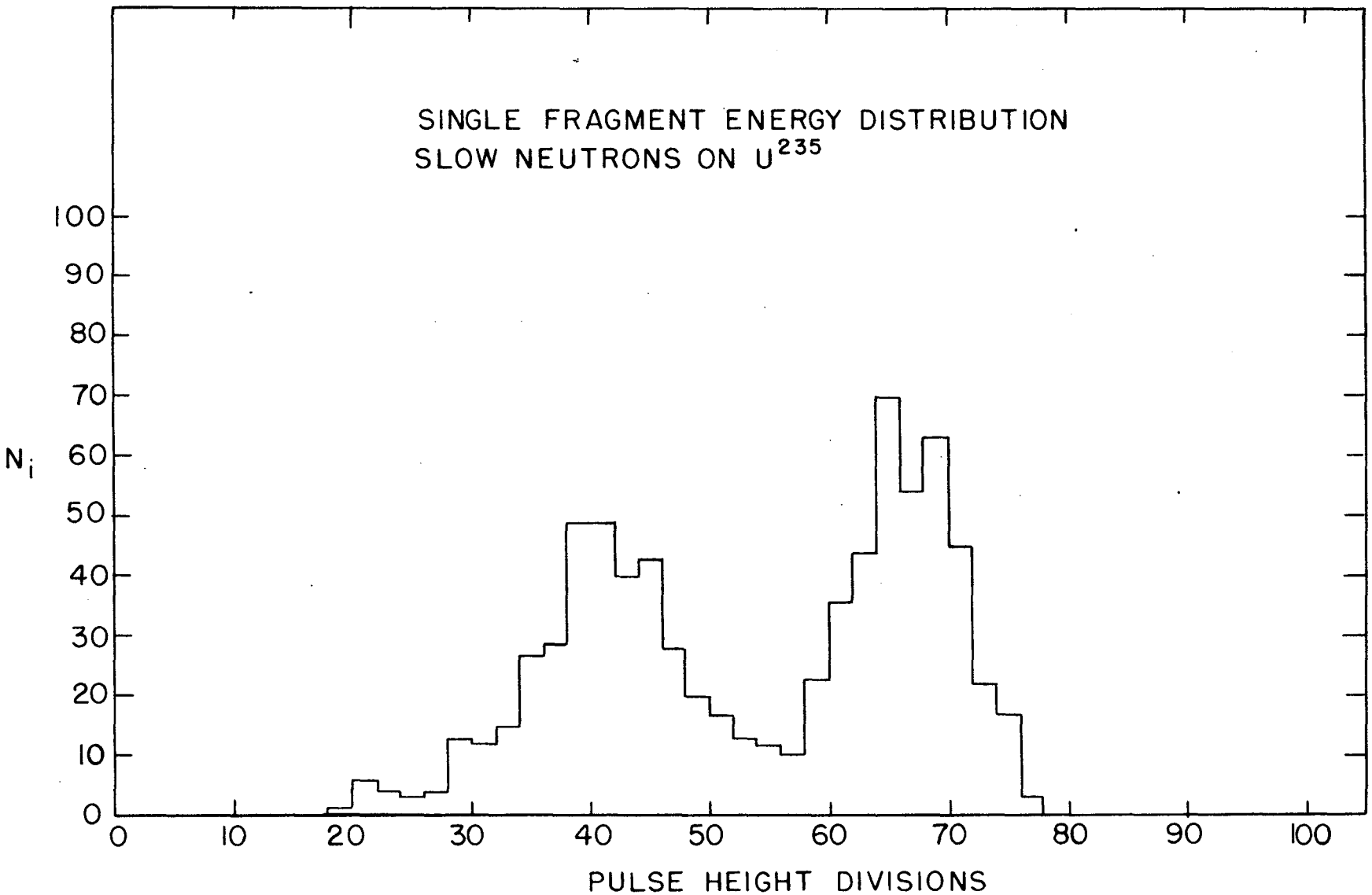
SINGLE FRAGMENT ENERGY DISTRIBUTION
SLOW NEUTRONS ON U^{235}
N_i
100
90
80
70
60
50
40
30
20
10
0
0
10
20
30
40
50
60
70
80
90
100
PULSE HEIGHT DIVISIONS

FIG. 11

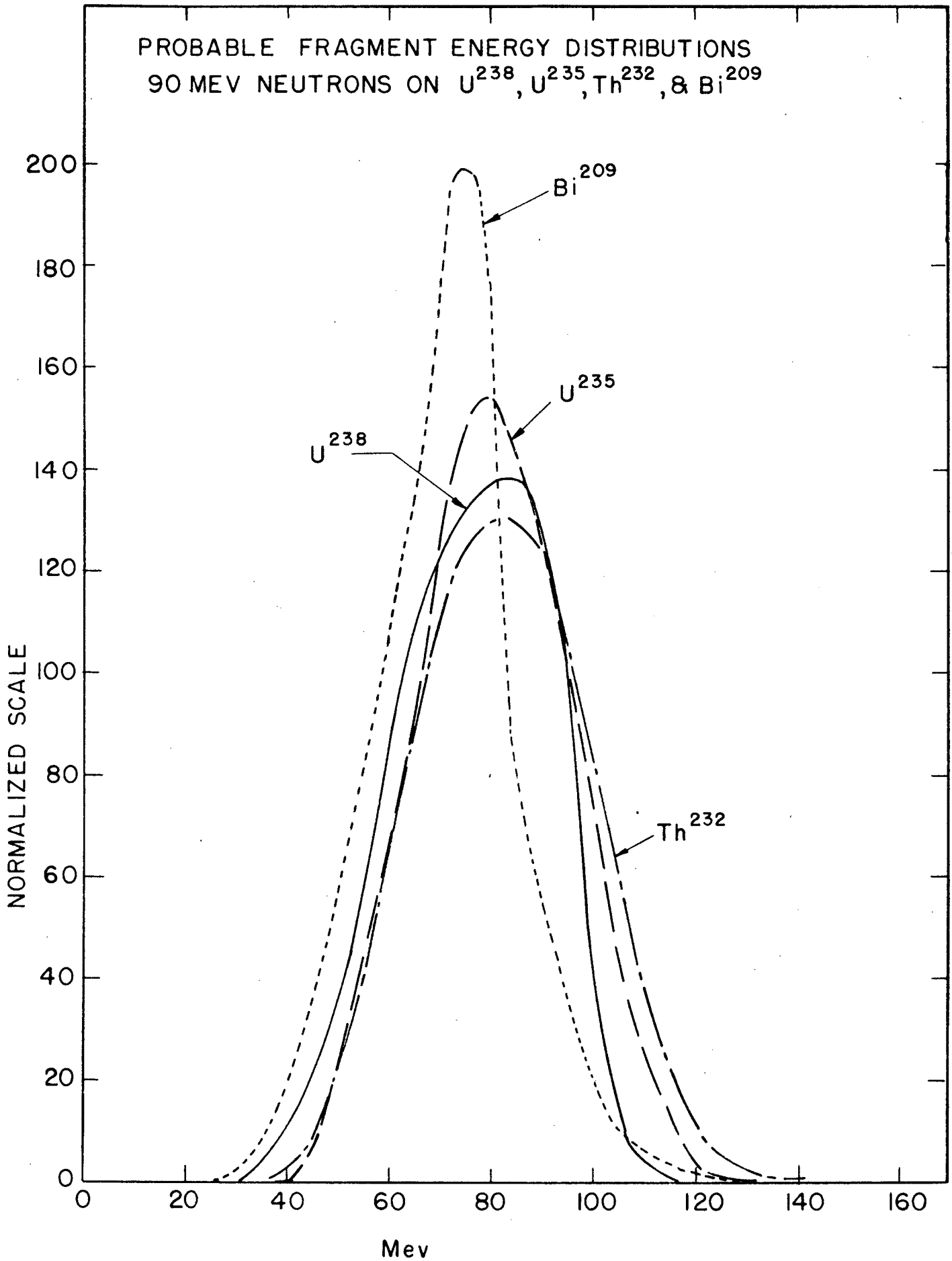

FIG. 12

13215-1

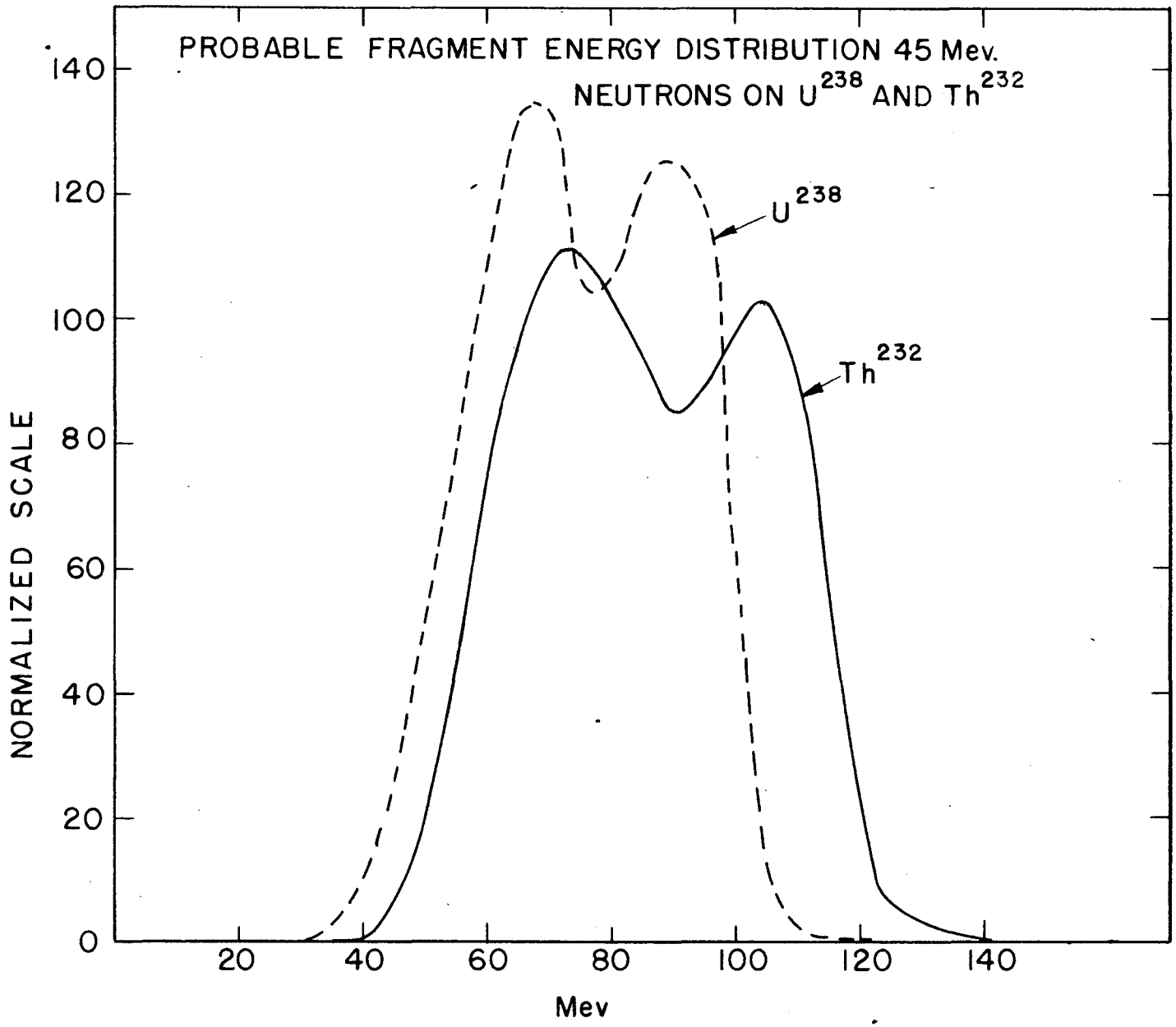
PROBABLE FRAGMENT ENERGY DISTRIBUTION 45 Mev.
NEUTRONS ON U238 AND Th232
U238
Th232
NORMALIZED SCALE
0
20
40
60
80
100
120
140
Mev

FIG. 13

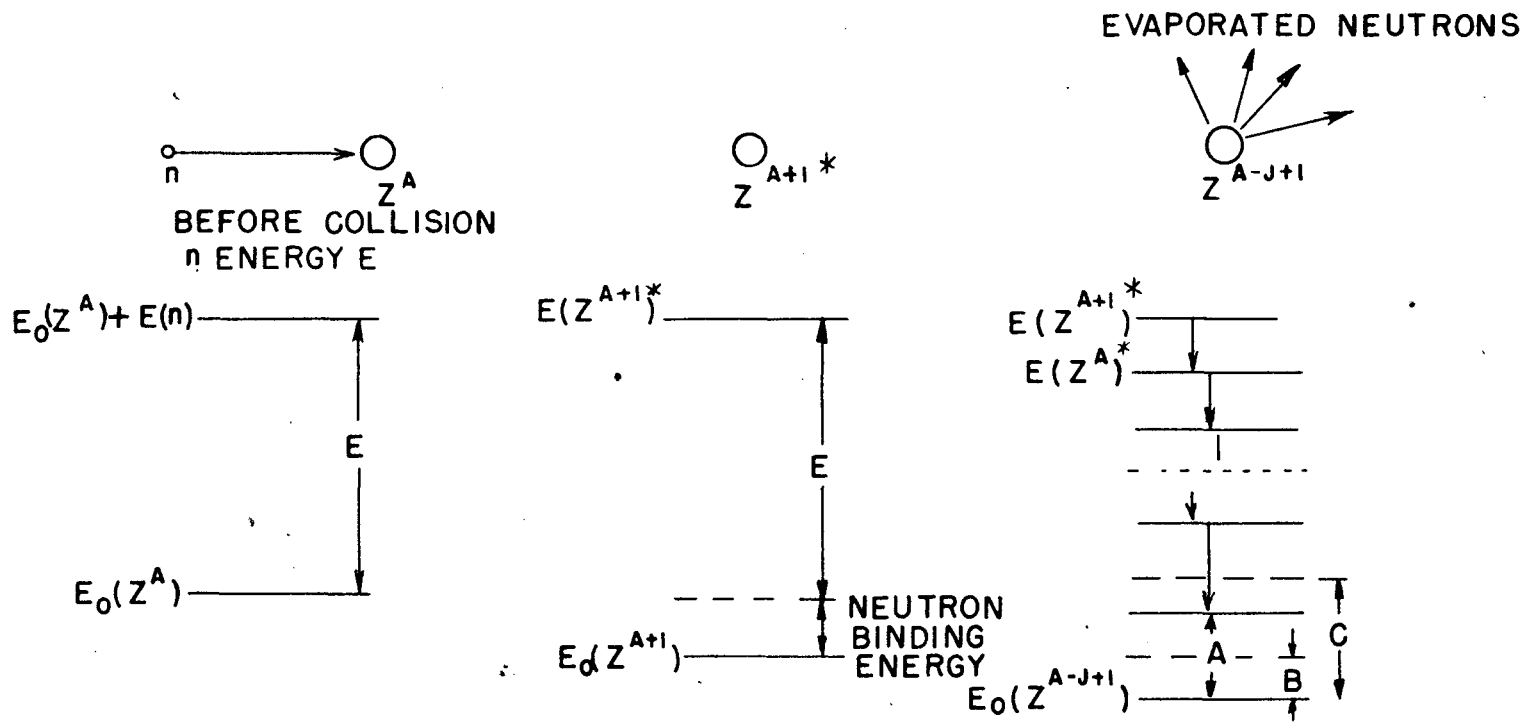
EVAPORATED NEUTRONS
n
Z^A
BEFORE COLLISION
n ENERGY E
Z^{A+1*}
Z^{A-J+1}
$E_0(Z^A) + E(n)$
E
$E_0(Z^A)$
$E(Z^{A+1*})$
E
NEUTRON
BINDING
ENERGY
$E_0(Z^{A+1})$
$E(Z^{A+1*})$
$E(Z^{A*})$
A
B
C
$E_0(Z^{A-J+1})$

FIG. 14

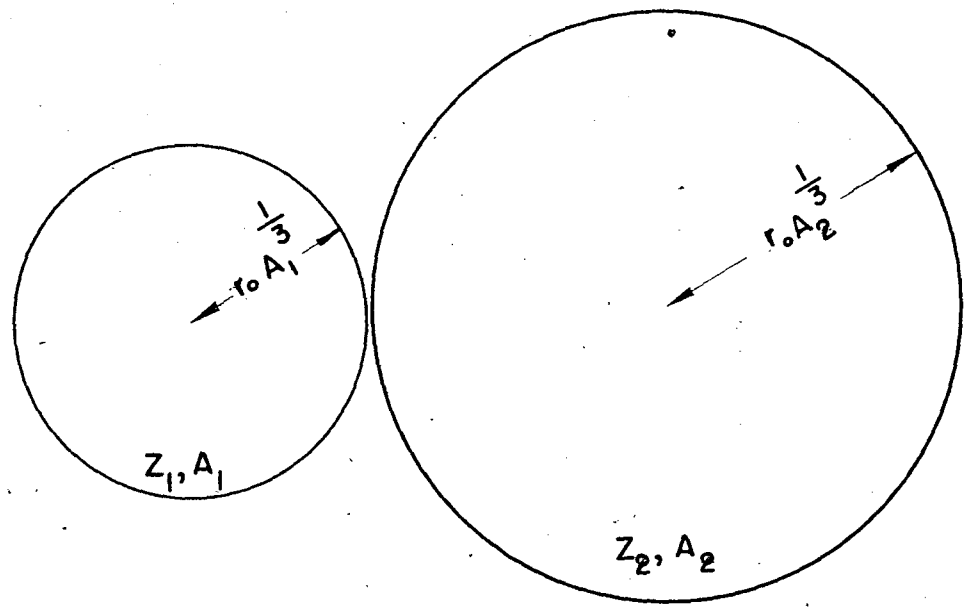

FIG. 15

DECLASSIFIED